Determining the refractive index and average thickness of AsSe semiconducting glass films from wavelength measurements only

C. Corrales, J. B. Ramírez-Malo, J. Fernández-Peña, P. Villares, R. Swanepoel, and E. Márquez

The dispersive refractive index $n(\lambda)$ and thickness d of chalcogenide glass thin films are usually calculated from measurements of both optical transmission and wavelength values. Many factors can influence the transmission values, leading to large errors in the values obtained for $n(\lambda)$ and d. A novel optical method is used to derive $n(\lambda)$ and d for AsSe semiconducting glass thin films deposited by thermal evaporation in the spectral region where $k^2 \ll n^2$, using only wavelength values. This entails obtaining two transmission spectra: one at normal incidence and another at oblique incidence. The procedure yields values for the refractive index and average thickness of thermally evaporated chalcogenide films to an accuracy better than 3%. © 1995 Optical Society of America

1. Introduction

Chalcogenide glasses are of considerable interest for use as optical elements in IR-transmitting applications because of their transparency over a wide wavelength range in the IR region, and a variety of possible applications can be envisaged depending on the wavelength of the light involved.[1] Cimpl and Kosek[2] have described the use of amorphous chalcogenide thin films as antireflection coatings for IR optics (e.g., filters), taking advantage of the fact that the refractive index can be varied over quite a wide range (2–3.5 for AsS and Te-based systems, respectively) by varying the composition so that a good match of the refractive index of film n with that of the optical element itself, n_1, can be achieved (for zero reflectivity), $n = n_1^{1/2}$. In addition, materials having high refractive indices such as chalcogenide glasses are candidates for exhibiting large third-order nonlinearities[3]; the nonlinear optical properties of materials are becoming increasingly important in high-power laser applications. It must be emphasized that the thickness and refractive index of the chalcogenide glass films are, obviously, of particular significance in most of their applications and can be determined in a nondestructive way from their optical transmission spectra.

The theory of the optical transmission of thin films on transparent substrates has been widely investigated.[4,5] Expressions for transmission T are usually complicated functions of refractive index n and film thickness d, and the treatment of these spectra involves elaborate computer procedures. Simple direct procedures have also been devised for $k^2 \ll n^2$. This involves the construction of continuous envelopes T_M and T_m around the maxima and minima of the interference fringes.[6–8] These optical procedures require extremely accurate experimental measurements using a small slit width and cannot often be done with a spectrophotometer. A more fundamental problem regarding these methods is that they are valid only for homogeneous films with uniform thickness. Even small inhomogeneities have a significant influence on the experimental values of T and can easily result in errors of as high as 100% for the calculated values of d. Methods have been devised to compensate for inhomogeneities, but this still requires accurate measurements of T.[9,11] The value of T is also a function of the substrate properties.

In contrast with the transmission, wavelength λ

C. Corrales is with the Departamento de Ingenieria de Sistemas y Automática, Facultad de Ciencias Náuticas, Universidad de Cádiz, Puerto Real, Cádiz, Spain. J. B. Ramirez-Malo, J. Fernández-Peña, P. Villares, and E. Márquez are with the Departamento de Fisica de la Materia Condensada, Facultad de Ciencias, Universidad de Cádiz, Puerto Real, Cádiz, Spain. R. Swanepoel is with the Department of Physics, Rand Afrikaans University, Johannesburg, South Africa.

Received 10 January 1995; revised manuscript received 5 June 1995.
0003-6935/95/347907-07$06.00/0.

can be accurately measured with a spectrophotometer. The wavelength of the interference maxima and minima can also be accurately determined. These values of λ are independent of factors that influence the values of T and have unique values even for inhomogeneous films.[9] Thus it would be helpful if n and d could be determined from measurements of λ alone, and methods to achieve this are used in this study.[12] The thin-film amorphous chalcogenide materials under study all belong to the AsSe binary system (the glassy compositions analyzed are Se, $As_{30}Se_{70}$, $As_{40}Se_{60}$, $As_{50}Se_{50}$, and $As_{60}Se_{40}$), and we focus mainly on two representative cases, namely, a-Se films and a-$As_{40}Se_{60}$ (As_2Se_3) films. To the best of our knowledge, this is the first time that the refractive index and thickness of chalcogenide glass thin films deposited by thermal evaporation can be determined using only wavelength measurements.

2. Theory

The basis of the analysis that follows is the assumption that a mathematical expression for dispersion $n(\lambda)$ exists. It is also assumed that n is isotropic. From the theory for normal dispersion[13] as well as from practical experience, it follows that the spectral dependence of the refractive index can be accurately represented by three constants, x, a, and b, in the region of $k^2 \ll n^2$ by an equation of the form

$$n^2 = \frac{a}{\lambda^x} + b. \quad (1)$$

For normal incidence on a film with thickness d one can obtain the wavelengths of the transmission extrema by the well-known expression

$$2n_0 d = m\lambda_0. \quad (2)$$

We consider only those cases when n is larger than the substrate refractive index and when m has integer values for the maxima and half-integer values for the minima.

The problem is thus reduced to determining five constants: m, d, x, a, and b from the transmission spectrum. Only m and x as well as the product $n_0 d$ can be determined solely from Eqs. (1) and (2); thus another experimental equation must be found to determine the other constants. This can be done by obtaining a second transmission spectrum at an angle of incidence $i > 0$ (see Fig. 1). The equation for the interference extrema now becomes[14]

$$2n_i d \cos r = m\lambda_i, \quad (3)$$

where r is the angle of refraction in the film. The five constants can now be found from Eqs. (1)–(3) in various ways, provided that at least three extrema are available.

In Fig. 2 the solid spectra show two typical transmission spectra for normal incidence in the transparent and absorption regions. The broken spectra represent two spectra of the same films at an incident angle of 30°, and all the spectra shift toward the shorter wavelength region according to Eq. (3).

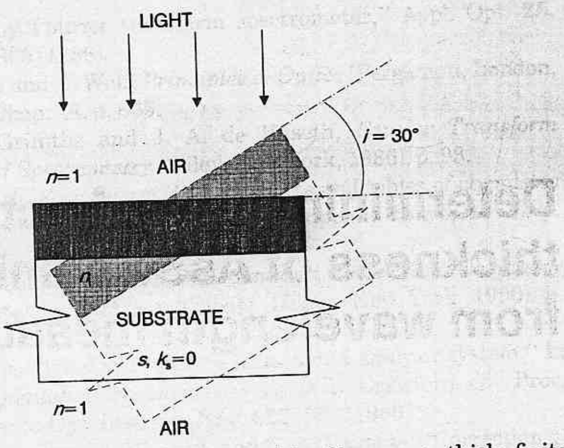

Fig. 1. System of an absorbing thin film on a thick finite transparent substrate.

A. Determining n from the Order Numbers m

We now consider m not to be a discrete-order numbe but a continuous mathematical variable. The spec trum for normal incidence can be shifted towar shorter wavelengths by increasing each order numbe by an amount Δm, where Δm can be different for eac m. The shifting that is due to oblique incidenc according to Eq. (3) can thus be written in terms o

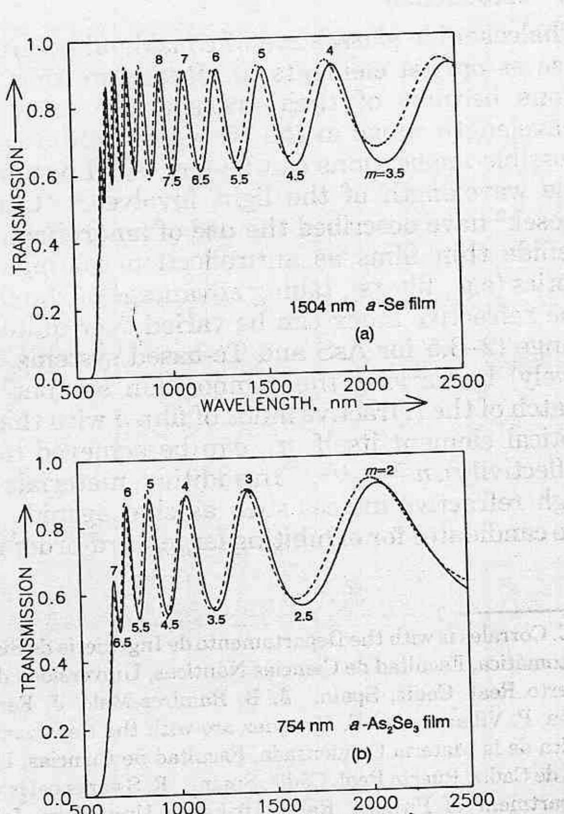

Fig. 2. Transmission spectra of thin films of (a) a-Se and a-As_2Se_3 on a glass substrate for normal incidence (solid curve) an angle of incidence of 30° (broken curve).

normal incidence as

$$2n_i d = (m + \Delta m)\lambda_i. \tag{4}$$

From Eqs. (3) and (4) and Snell's law it follows that

$$\cos r = \frac{m}{m + \Delta m}, \tag{5}$$

$$n_i = \frac{\sin i}{\sin r}. \tag{6}$$

Considering two adjacent extrema of the normal-incidence spectrum at wavelengths λ_{01} and λ_{02} from Eq. (2) it follows that

$$m_1 = \frac{n_{01}\lambda_{02}}{2(n_{02}\lambda_{01} - n_{01}\lambda_{02})}.$$

The quantity M is now defined as

$$M = \frac{\lambda_{02}}{2(\lambda_{01} - \lambda_{02})}, \tag{7}$$

where $M \geq m_1$. The equality $M = m_1$ is true only in the absence of dispersion. The effect of dispersion on M can be approximated by a mathematical function of the form

$$M = \frac{C}{\lambda_0}\left(1 + \frac{D}{\lambda_0^{\,y}}\right). \tag{8}$$

The first term in Eq. (8) reflects the $1/\lambda$ relation between m and λ according to Eq. (2), whereas the term in parentheses approximates the effect of dispersion. The value of m at each extremum is now approximately given by $m \approx C/\lambda_0$. Equation (8) can be rewritten in the form of an equation for a straight line:

$$M\lambda_0 = \frac{DC}{\lambda_0^{\,y}} + C. \tag{9}$$

The value of y can be determined by iterating y and performing a linear regression of Eq. (9). The value of y is chosen such that it gives a good fit to Eq. (9) and yields values of m according to the approximation $m \approx C/\lambda_0$, which differs by 1/2, and also yields correct approximate integer or half-integer values for each corresponding extremum—from the approximate values of m exact-order numbers can now be assigned to each extremum.

Substitution of Eq. (1) into Eq. (2) yields

$$m^2\lambda_0^{\,2} = \frac{A}{\lambda_0^{\,x}} + B, \tag{10}$$

where $A = 4ad^2$ and $B = 4bd^2$. Since the order numbers are known, the value of x can be determined by iteration and by performing a linear regression of Eq. (10). The value of x that gives the best fit to experimental values is chosen, and the regression also yields the values of A and B.

Substituting Eq. (1) into Eq. (4), using Eq. (10), and solving for Δm yield

$$\Delta m = \left[m^2\frac{\lambda_0^{\,2}}{\lambda_i^{\,2}} + \frac{A}{\lambda_i^{\,2}}\left(\frac{1}{\lambda_i^{\,x}} - \frac{1}{\lambda_0^{\,x}}\right)\right]^{1/2} - m. \tag{11}$$

The value of n_i at each value of λ_i can now be calculated using Eqs. (11), (5), and (6).

The value of d can be determined by using the fact that m increases by 1/2 for each successive extremum described by Eq. (4). If m_1 is the order number of the first extremum considered at the long-wavelength end, Eq. (4) can be rewritten for the successive extrema as

$$\frac{j}{2} + \Delta m = 2d\frac{n_i}{\lambda_i} - m_1, \tag{12}$$

where $j = 0, 1, 2, 3, \ldots$. Equation (12) can be plotted as shown in Fig. 3. A straight line through $-m_1$ and the other points has a slope $2d$, and the value of d can be obtained from this slope. With d known, a and b can be calculated from Eq. (10), which completes the calculation of the required five constants.

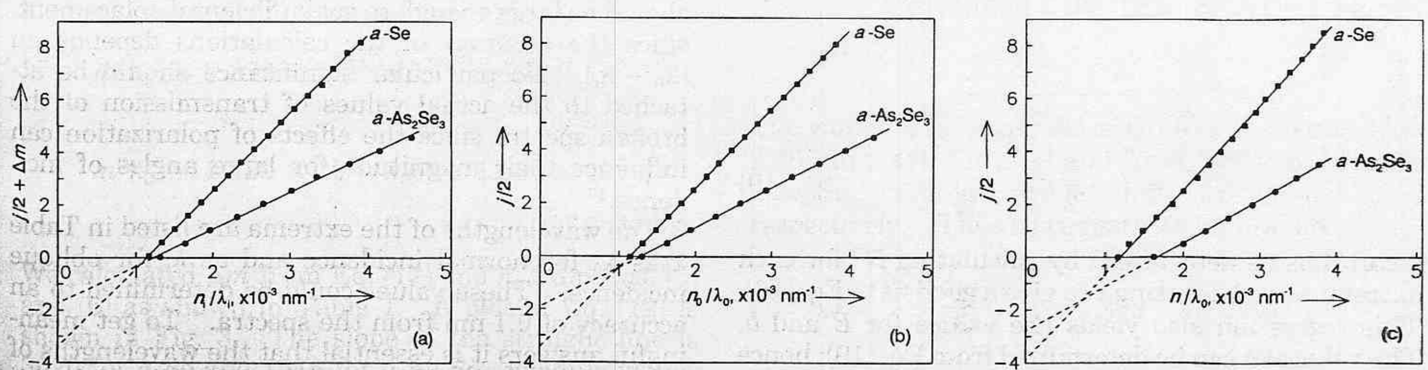

Fig. 3. Plots of (a) n_i/λ_i versus $j/2 + \Delta m$, (b) n_0/λ_0 versus $j/2$, and (c) n/λ_0 versus $j/2$ for a-Se and a-As_2Se_3 thin films to determine the thickness of film d.

B. Determining n from the Dispersion Equation

An alternative way of calculating n independent from m is now considered. From Eqs. (2) and (3) it follows that

$$n_i \cos r = n_0 \frac{\lambda_i}{\lambda_0}. \quad (13)$$

In a nondispersive case Eq. (13) becomes $\cos r = (\lambda_i/\lambda_0)$, and n can be calculated directly from Eq. (6).

Equation (13) can be rewritten as

$$n_i^2(1 - \sin^2 r) = n_0^2 \frac{\lambda_i^2}{\lambda_0^2}.$$

Substituting Eq. (6) into the above equation yields

$$n_i^2 - n_0^2 \frac{\lambda_i^2}{\lambda_0^2} = \sin^2 i. \quad (14)$$

On the other hand, from Eq. (1), by expanding n_i^2 in a Taylor series around n_0, it follows that

$$n_i^2 = n_0^2 + \frac{ax}{\lambda_0^{x+1}}(\lambda_0 - \lambda_i). \quad (15)$$

Substituting Eq. (15) into Eq. (14) yields

$$n_0^2 = N^2 - \frac{ax}{\lambda_0^{x-1}(\lambda_0 + \lambda_i)}, \quad (16)$$

where

$$N^2 = \frac{\lambda_0^2 \sin^2 i}{\lambda_0^2 - \lambda_i^2}. \quad (17)$$

Equations (1) and (16) show that N^2 can also be represented by a function of the form

$$N^2 = \frac{E}{\lambda^x} + b. \quad (18)$$

From Eqs. (1), (18), and (16) it follows that

$$\frac{E}{a} = \frac{(1 + x)\lambda_0 + \lambda_i}{\lambda_0 + \lambda_i} \approx 1 + \frac{x}{2}. \quad (19)$$

x can thus be determined by calculating N^2 for each extremum and iterating x to give a good fit to Eq. (18). This regression also yields the values for E and b. The value of a can be determined from Eq. (19); hence one can determine $n(\lambda)$.

To determine m and d we can write an equation similar to Eq. (12):

$$\frac{j}{2} = 2d \frac{n_0}{\lambda_0} - m_1. \quad (20)$$

Values of $j/2$ are now plotted as functions of n_0/λ_0 as shown in Fig. 3. Extrapolation of a straight line through these points indicates the order number of the first extremum, m_1. A straight line through $-m_1$ and the points again has a slope $2d$ from which d can be determined. This completes the calculation of the required five constants.

3. Experimental Results and Discussion

Figure 2 shows the optical transmission spectra obtained from thin films of a-Se and a-As_2Se_3 deposited upon room-temperature substrates (glass microscope slides). The glass films were deposited by vacuum evaporation in a conventional coating unit (Edwards Model E306A) at a pressure $<10^{-6}$ Torr from a quartz crucible. Electron microprobe analysis of the as-deposited AsSe films indicates that the stated composition is correct to ± 1 at. %. Care was taken during sample preparation to minimize exposure to light sources, and the samples were kept in complete darkness until required. Photodarkening is a light-induced effect that occurs in chalcogenide glasses[15]: it results in a significant increase of the refractive index. The structure and properties of amorphous chalcogenide films are known to be strongly affected by the deposition rate,[16] which in this study is within the range of 1–2 nm s^{-1}, and was continuously measured using the quartz crystal microbalance technique (Edwards Model FTM-5). The lack of crystallinity in the AsSe films was verified by x-ray diffraction analysis. The thin-film sample was mounted on an accurate goniometer installed in the sample compartment of a double-beam, ratio-recording UV/vis/near-IR computer-controlled spectrophotometer (Perkin-Elmer Model Lambda-19). The wavelength range studied was from 0.3 to 2.5 μm.

The solid spectra in Fig. 2 represent the spectra for normal incidence, whereas the broken spectra are for an angle of incidence of $i = 30.0°$. The slit of the instrument was set at 1 nm. The angle of incidence should be large enough to get sufficient displacement since the accuracy of the calculations depends on $(\lambda_0 - \lambda_i)$. No particular significance should be attached to the actual values of transmission of the broken spectra since the effects of polarization can influence their magnitude for large angles of incidence.[17]

The wavelengths of the extrema are listed in Table 1 as λ_0 for normal incidence and as λ_i for oblique incidence. These values could be determined to an accuracy of 0.1 nm from the spectra. To get meaningful answers it is essential that the wavelengths of the extrema be determined to an accuracy of better than 1 nm. The values of M that were calculat

Table 1. Calculations for the Refractive Index of a-Se and a-As_2Se_3 Thin Films Prepared by Thermal Evaporation

Sample	λ_0	λ_i	M	m_y	m	Δm	n_i	N	n_0	n	T_M	T_m	n_T
a-Se	2123.3	2078.7	3.5	3.5	3.5	0.0759	2.440	2.452	2.434	2.472	0.916	0.617	2.467
	1861.1	1822.4	4.1	4.0	4.0	0.0863	2.446	2.465	2.439	2.476	0.915	0.617	2.469
	1657.0	1622.8	4.7	4.5	4.5	0.0970	2.447	2.474	2.446	2.480	0.913	0.617	2.470
	1496.7	1466.4	5.2	5.0	5.0	0.1065	2.461	2.498	2.454	2.489	0.911	0.614	2.487
	1364.9	1337.8	5.7	5.5	5.5	0.1159	2.474	2.522	2.464	2.497	0.909	0.611	2.531
	1255.5	1231.2	6.4	6.0	6.0	0.1246	2.492	2.554	2.475	2.505	0.908	0.608	2.516
	1165.0	1143.0	7.0	6.4	6.5	0.1332	2.508	2.585	2.488	2.518	0.906	0.605	2.532
	1087.7	1067.7	7.4	6.9	7.0	0.1415	2.524	2.619	2.502	2.532	0.905	0.603	2.529
	1019.2	1000.9	8.3	7.4	7.5	0.1503	2.535	2.650	2.518	2.542	0.905	0.601	2.539
	961.1	944.4	8.8	7.8	8.0	0.1575	2.557	2.694	2.536	2.557	0.905	0.599	2.540
	909.5	894.2	9.6	8.3	8.5	0.1648	2.576	2.737	2.555	2.571	0.905	0.597	2.545
	864.5	850.4	10.6	8.7	9.0	0.1721	2.593	2.780	2.575	2.588	0.904	0.599	2.541
	825.6	812.7	11.1	9.1	9.5	0.1770	2.626	2.840	2.597	2.608	0.907	0.601	2.526
	790.0	778.1	12.5	9.5	10.0	0.1830	2.650	2.892	2.619	2.627	0.909	0.597	2.542
	759.5	748.3	13.0	9.9	10.5	0.1913	2.655	2.922	2.642	2.652	0.908	0.591	2.559
	731.3	721.0	14.0	10.3	11.0	0.1949	2.692	2.990	2.667	2.675	0.905	0.585	2.578
	706.1	696.5	—	10.6	11.5	0.2001	2.715	3.043	2.691	2.701	0.889	0.575	2.585
a-As_2Se_3	2047.8	2011.5	2.0	2.0	2.0	0.0366	2.649	2.667	2.659	2.715	0.916	—	—
	1643.5	1614.9	2.7	2.5	2.5	0.0455	2.657	2.692	2.668	2.724	0.908	0.556	2.680
	1388.3	1364.9	3.1	3.0	3.0	0.0537	2.678	2.735	2.682	2.761	0.902	0.551	2.761
	1194.0	1174.8	3.8	3.5	3.5	0.0611	2.710	2.799	2.703	2.770	0.895	0.547	2.725
	1056.1	1040.1	4.4	3.9	4.0	0.0675	2.756	2.883	2.732	2.801	0.889	0.542	2.724
	947.5	934.2	5.2	4.4	4.5	0.0725	2.819	2.995	2.771	2.827	0.884	0.538	2.748
	864.2	852.7	5.9	4.8	5.0	0.0788	2.849	3.075	2.817	2.865	0.879	0.533	2.751
	796.5	787.0	7.1	5.2	5.5	0.0803	2.959	3.247	2.873	2.904	0.873	0.527	2.758
	744.3	736.2	7.5	5.6	6.0	0.0822	3.051	3.398	2.933	2.961	0.862	0.513	2.793
	697.9	691.0	—	5.9	6.5	0.0836	3.147	3.565	3.003	3.007	0.769	0.489	2.743

from Eq. (7) using the values of λ_0 in pairs are also shown in Table 1. We fit these values to Eq. (9) by iterating y in steps of 0.1 from 1 to 7. A good fit was obtained for the value of $y = 3.4$ in the case of a-Se and $y = 3.0$ in the case of a-As_2Se_3, yielding

$$M\lambda_0 = 1.498 \times 10^{13}/\lambda_0^{3.4} + 7.510 \quad \text{for } a\text{-Se},$$

$$M\lambda_0 = 6.524 \times 10^{11}/\lambda_0^{3.0} + 4.144 \quad \text{for } a\text{-As}_2\text{Se}_3.$$

The values of m calculated from the expression $m \approx C/\lambda_0$ are shown as m_y in Table 1. These values are, of course, only approximate but serve to assign the actual values of m to each extremum as shown in Table 1. We used the correct values of m in Eq. (10), iterating x in steps of 0.1 from 1 to 7. The best fit was obtained for $x = 3.1$ in the case of a-Se and $x = 3.0$ in the case of a-As_2Se_3, yielding

$$m^2\lambda_0^2 = 7.372 \times 10^{15}/\lambda_0^{3.1} + 5.491 \times 10^7 \quad \text{for } a\text{-Se},$$

$$m^2\lambda_0^2 = 1.320 \times 10^{15}/\lambda_0^{3.0} + 1.667 \times 10^7 \quad \text{for } a\text{-As}_2\text{Se}_3.$$

We calculated Δm from Eq. (11) and n_i from Eqs. (5) and (6) as shown in Table 1. A plot of Eq. (12) is shown in Fig. 3. The slope of the straight line is 3020 for a-Se and 1516 for a-As_2Se_3, yielding values for d of 1510 and 758 nm, respectively. The constants a and b were calculated from Eq. (10), yielding the following equations for $n(\lambda)$:

$$n^2 = \frac{8.084 \times 10^8}{\lambda^{3.1}} + 6.022 \quad \text{for } a\text{-Se}, \tag{21}$$

$$n^2 = \frac{5.743 \times 10^8}{\lambda^{3.0}} + 7.253 \quad \text{for } a\text{-As}_2\text{Se}_3. \tag{22}$$

Following the second procedure, we calculated the values of N^2 from Eq. (17), which are shown as N in Table 1. A least-squares fit of Eq. (18) yields the best values of $x = 2.9$ for a-Se and $x = 3.7$ for a-As_2Se_3:

$$N^2 = \frac{6.192 \times 10^8}{\lambda^{2.9}} + 5.868 \quad \text{for } a\text{-Se},$$

$$N^2 = \frac{1.891 \times 10^{11}}{\lambda^{3.7}} + 7.036 \quad \text{for } a\text{-As}_2\text{Se}_3.$$

The values of E/a calculated from Eq. (19) vary from 2.465 to 2.460 for a-Se and from 2.867 to 2.859 for a-As_2Se_3, yielding average values of 2.463 and 2.863, respectively. Thus the equations for $n(\lambda)$ are

$$n^2 = \frac{2.514 \times 10^8}{\lambda^{2.9}} + 5.868 \quad \text{for } a\text{-Se}, \tag{23}$$

$$n^2 = \frac{6.604 \times 10^{10}}{\lambda^{3.7}} + 7.036 \quad \text{for } a\text{-As}_2\text{Se}_3. \tag{24}$$

A plot of Eq. (20), shown in Fig. 3, yields the value of the first-order number as 3.5 and a slope of 2994 for a-Se and 2.0 and 1500 for a-As_2Se_3, yielding values for d of 1497 and 750 nm, respectively.

Taking average values for d of 1504 and 754 nm, one can now finally calculate n from m and d using Eq. (2). These values are shown in Table 1. A fit of these final values to Eq. (1) yields

$$n^2 = \frac{8.154 \times 10^8}{\lambda^{3.1}} + 6.074 \quad \text{for } a\text{-Se}, \qquad (25)$$

$$n^2 = \frac{5.802 \times 10^8}{\lambda^{3.0}} + 7.328 \quad \text{for } a\text{-As}_2\text{Se}_3. \qquad (26)$$

The agreement between the two methods is excellent. The differences between the thicknesses determined through each of the proposed methods are 13 and 8 nm, respectively. The values of n that correspond to a-Se calculated by Eqs. (21), (23), and (25) agree to an accuracy of better than 2% from the infinite-wavelength region to 600 nm, whereas in the case of a-As_2Se_3, Eqs. (22), (24), and (26) agree to an accuracy of better than 3%.

The values of $n(\lambda)$ obtained from λ alone are now compared with those obtained from the transmission values. Continuous envelopes T_M and T_m were constructed around the maxima and minima of the interference fringes of the normal-incidence spectra shown in Fig. 2.[18] The values of T_M and T_m for each fringe are shown in Table 1. If the substrate refractive index is $s(\lambda)$, the value of n is given by[7]

$$n^2 = P + (P^2 - s^2)^{1/2}, \qquad (27)$$

where

$$P = 2s\,\frac{T_M - T_m}{T_M T_m} + \frac{s^2 + 1}{2}.$$

The values of n calculated from Eq. (27) are shown as n_T in Table 1. On the other hand, a plot of Eq. (20) using the values of n_T yields a value for d of 1599 nm in the case of a-Se and a value of 814 nm in the case of a-As_2Se_3 (see Fig. 3). In the case of nonuniform thermally evaporated films the transmission spectra shrink considerably and then yield values of T_M that are too small and values of T_m that are too large. Equation (27) then yields values of n that are too small and a value for d from Eq. (20) that is too large.[19] In the a-Se film under study it was found that, for $\lambda \leq 1000$ nm, the refractive index obtained by Eq. (27) is lower than the one derived only from the wavelength measurements, and the film thickness determined from the transmission measurements turns out to be 6% higher. In the a-As_2Se_3 film, the refractive index n_T is remarkably lower throughout the spectral range, and the corresponding thickness is 8% higher. Interestingly, these results mean that the a-As_2Se_3 film is slightly less uniform in its thickness than the a-Se film.

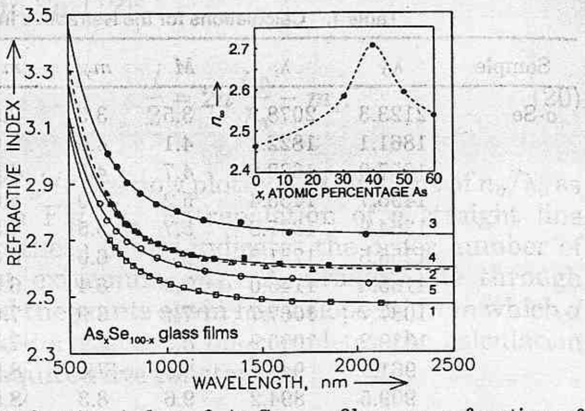

Fig. 4. Refractive index of As_xSe_{100-x} films as a function of wavelength for various values of x: curve 1, $x = 0$; curve 2, $x = 30$; curve 3, $x = 40$; curve 4, $x = 50$; curve 5, $x = 60$. The inset shows the refractive index of As_xSe_{100-x} films at $E = 0$ (infinite-wavelength refractive index n_∞) as a function of x.

We used a stylus-based surface profiler (Sloan Model Dektak IIA) to determine the thickness of the films for comparison with the results derived from the wavelength measurements. The values of d in the same areas of the films for a-Se and a-As_2Se_3 were 1483 ± 30 nm and 742 ± 15 nm, respectively, showing good agreement with those determined with the optical procedure—the difference in both cases is less than 2%. Furthermore, the final refractive-index values for a-Se show differences of less than 3% for $\lambda \geq 600$ nm, according to the refractive-index data reported by Koehler *et al.* in Wemple[20] As for the n values of the glassy composition As_2Se_3, Ohmachi[21] reported refractive-index data that differ from ours by less than 6% for $\lambda \geq 600$ nm. (It should be mentioned that Ohmachi's specimen was annealed at approximately 160 °C in air and cooled slowly to room temperature over seven days.) De Neufville *et al.*[22] reported a value of 2.77 ± 0.05 measured at a photon energy of 1.0 eV (1240 nm), which is indeed very close to the 2.763 derived from Eq. (26).

Figure 4 shows the n values for the rest of the glassy compositions in the AsSe binary semiconducting system under study: $As_{30}Se_{70}$, $As_{50}Se_{50}$, and $As_{60}Se_{40}$, together with their respective fits to Eq. (1). It must be emphasized that the compositional dependence of the refractive index is in excellent agreement with that reported by Lucovsky[23] for AsSe bulk glass samples. [The values of the refractive index were obtained from a reflectance measurement in the transparent regime at ~1000 cm^{-1} (10 μm) and show a maximum in the stoichiometric composition $As_{40}Se_{60}$.]

4. Concluding Remarks

In summary, for inhomogeneous or nonuniform thin films Eq. (27) yields answers that are more or less inaccurate, whereas the procedure that we have described (and successfully applied to wedge-shaped thin films of the AsSe semiconducting glass system prepared by thermal evaporation) using only the values of λ still yields the correct values for $n(\lambda)$ and d—inhomogeneities or nonuniformity do not affect the wavelength values of the optical interference extrema.

We can conclude that accurate measurement of absolute transmission T is relatively difficult in spectrophotometry. One can usually calculate the values of $n(\lambda)$ and d using the values of both T and λ. By obtaining a second transmission spectrum at oblique incidence we were able to present a method that can be used to calculate accurately the refractive index and average thickness of chalcogenide glass thin films. · We checked on complete correction when this optical procedure was used with some glassy compositions of the AsS and GeSe binary systems. Measurement of the absolute optical transmission is not necessary.

The authors are grateful to J. Reyes, L. Díaz, and R. Jiménez for their many valuable discussions. This study has been financially supported by grants from the Spanish Ministry of Education and Science.

References

1. S. R. Elliott, "Measurement of Optical Constants of Thin Films," in *Glasses and Amorphous Materials,* J. Zarzycki, ed. (VCH, Weinheim, Germany, 1991), p. 375.
2. Z. Cimpl and F. Kosek, "Utilization of chalcogenide glasses in infrared optics," J. Non-Cryst. Solids **90,** 577–580 (1987).
3. E. Hajto, P. J. S. Ewen, and A. E. Owen, "Linear and nonlinear optical properties of chalcogenide glasses," J. Non-Cryst. Solids **164–166,** 901–904 (1993).
4. O. S. Heavens, "Clalcogenide Glasses," in *Physics of Thin Films,* G. Hass and R. E. Thun, eds. (Academic, New York, 1964), Vol. 2, p. 193.
5. M. M. Koltun, *Selective Optical Surfaces for Solar Energy Converters* (Allerton, New York, 1981), p. 9.
6. J. C. Manifacier, J. Gasiot, and J. P. Fillard, "A simple method for the determination of the optical constants n, k and the thickness of weakly absorbing film," J. Phys. E **9,** 1002–1004 (1976).
7. R. Swanepoel, "Determination of the thickness and optical constants of amorphous silicon," J. Phys. E **16,** 1214–1222 (1983).
8. E. Márquez, J. B. Ramírez-Malo, P. Villares, R. Jiménez-Garay, P. J. S. Ewen, and A. E. Owen, "Calculation of the thickness and optical constants of amorphous arsenic sulphide films from their transmission spectra," J. Phys. D **25,** 535–541 (1992).
9. R. Swanepoel, "Determination of the surface roughness and optical constants of inhomogeneous amorphous silicon films," J. Phys. E **17,** 896–903 (1984).
10. E. Márquez, J. B. Ramírez-Malo, J. Fernández-Peña, R. Jiménez-Garay, P. J. S. Ewen, and A. E. Owen, "On the optical properties of wedge-shaped thin films of Ag-photodoped $As_{30}S_{70}$ glass," Opt. Mater. **2,** 143–150 (1993).
11. C. Corrales, "Optical properties and photoinduced effects in thin films of the As-Se glassy semiconducting system," Ph.D. dissertation (Departamento de Estructura y Propiedades de los Materiales, Universidad de Cádiz, Cádiz, Spain, 1994).
12. R. Swanepoel, "Determining refractive index and thickness of thin films from wavelength measurements only," J. Opt. Soc. Am. A **2,** 1339–1343 (1985).
13. F. S. Crawford, *Waves* (McGraw-Hill, New York, 1968), p. 152.
14. A. Nussbaum and R. A. Phillips, *Contemporary Optics for Scientists and Engineers* (Prentice-Hall, Englewood Cliffs, N.J., 1976), p. 168.
15. G. Pfeiffer, M. A. Paesler, and S. C. Agarwal, "Reversible photodarkening of amorphous arsenic chalcogens," J. Non-Cryst. Solids **130,** 111–143 (1991).
16. K. White, B. Kumar, and A. K. Rai, "Effect of deposition rate on structure and properties of As_2S_3 film," Thin Solid Films **161,** 139–147 (1988).
17. G. R. Fowles, *Introduction to Modern Optics* (Holt, Rinehart & Winston, New York, 1975), p. 44.
18. M. McClain, A. Feldman, D. Kahaner, and X. Ying, "An algorithm and computer program for the calculation of envelope curves," Comput. Phys. **5,** 45–48 (1991).
19. E. Márquez, J. B. Ramírez-Malo, P. Villares, R. Jiménez-Garay, and R. Swanepoel, "Optical characterization of wedge-shaped thin films of amorphous arsenic trisulphide based only on their shrunk transmission spectra," Thin Solid Films **254,** 83–91 (1995).
20. S. H. Wemple, "Refractive-index behavior of amorphous semiconductors and glasses," Phys. Rev. B **7,** 3767–3777 (1973).
21. Y. Ohmachi, "Refractive index of vitreous As_2Se_3," J. Opt. Soc. Am. **63,** 630–631 (1973).
22. J. P. De Neufville, S. C. Moss, and S. R. Ovshinsky, "Photostructural transformations in amorphous As_2Se_3 and As_2S_3 films," J. Non-Cryst. Solids **13,** 191–223 (1973/74).
23. G. Lucovsky, "Average energy gaps in the binary glass-alloy systems: $Ge_{1-x}Se_x$ and $As_{1-x}Se_x$," Phys. Rev. B **15,** 5761–5768 (1977).